New Promising Modified Activated Carbons for CH4 and CO2 Adsorption

Preprint · November 2023

CITATIONS
0

READS
14

6 authors, including:

Grace Iragena Dushime
Université de Pau et des Pays de l'Adour
4 PUBLICATIONS **0** CITATIONS
SEE PROFILE

Julie Bachelart
Université de Pau et des Pays de l'Adour
6 PUBLICATIONS **2** CITATIONS
SEE PROFILE

Khaled Abou Alfa
Université de Pau et des Pays de l'Adour
5 PUBLICATIONS **5** CITATIONS
SEE PROFILE

Camelia Matei Ghimbeu
French National Centre for Scientific Research
162 PUBLICATIONS **4,957** CITATIONS
SEE PROFILE

New Promising Modified Activated Carbons for CH_4 and CO_2 Adsorption

G Iragena Dushime[1*], J Bachelart[1], K Abou Alfa[1], C Matei Ghimbeu[2], C Hort[1] and V Platel[1]

[1] Université de Pau et des Pays de l'Adour / E2S UPPA, Laboratoire de Thermique, Energetique et Procedes, EA1932, 64000 Pau, France.
[2] Institut de Sciences des Matériaux de Mulhouse, CNRS UMR 7361 UHA, 15 rue Jean Starcky, 68057 Mulhouse, France
grace.iragena-dushime@univ-pau.fr

Abstract. This work focuses on methane (CH_4) and carbon dioxide (CO_2) pure gases adsorption using commercial activated carbon (CNR-115), and its modified activated carbons: the one obtained via oxidation (CNR-115-ox) and the other given by oxidation followed by ammonium impregnation (CNR-115-ox-am). A homemade setup was used for isotherms determination at 303.15K and 0 - 3MPa. At 3MPa, CO_2 and CH_4 uptakes were: CNR-115 (12.05 mmol/g and 5.18 mmol/g respectively) > CNR-115-ox (7.79 mmol/g and 3.16 mmol/g respectively) > CNR-115ox-am (4.05 mmol/g and 1.53 mmol/g respectively). Hence: a) CNR-115 with high BET surface area (1714 m^2/g) adsorbs higher amount of gases than CNR-115-ox (929 m^2/g), which also adsorbs more gases than CNR-115-ox-am with the least BET surface area (352 m^2/g), and b) CO_2 with smaller molecular size (330pm) is more adsorbed on activated carbons surface than CH_4 (380pm). Further, the Langmuir model was used for adsorption description and the results are well comparable to the ones reported in the literature. Lastly, an interesting side of CNR-115-ox-am was discussed, and this activated carbon was found to be promising for CH_4 enrichment from CH_4/CO_2 mixtures due to its low CH_4 uptake.

Keywords: Activated carbons, adsorption, carbon dioxide, methane.

1 Introduction

The global world climate change and energy sector development are two main keys factors to promote the use of renewable energies. Historically, the use of gas for energy production began at the end of the 19th century. The sector was then improved and underwent many transformations [1]. Indeed, the first-generation gas called the city gas was obtained from coal pyrolysis and was then replaced by natural gas due to the fact that, the latter is naturally formed in some porous rocks and extracted by drilling instead of pyrolysis which also requires the use of energy. Currently, biogas (i.e. the third generation gas) is gaining too much attention over coal and natural gas because the former is a renewable energy contributing in climate protection by reducing the

emissions of greenhouse gases such as carbon dioxide (CO_2) [2]. Biogas (i.e. The mixture of CH_4 (30 - 75%) and CO_2 (15 - 50 %)) is produced from a process called anaerobic digestion through biochemical degradation of organic wastes materials [3]. However, the presence of carbon dioxide is not crucial for the use of biogas, as it lowers its heating value. This is the main reason of upgrading the biogas in order to produce biomethane which can therefore be used: i) for energy production, ii) as fuel for vehicles, and iii) natural gas pipelines injection. Concerning pipelines injection of biomethane, the gas must fit pipelines-quality requirements (i.e. $CO_2 < 3\%$, and $CH_4 > 97\%$) [4]. Biomethane is almost similar to natural gas in terms of calorific heat (> 8.55 and 11.4 kWh/Nm^3 for biomethane and natural gas respectively [5]), the difference between them is based on CO_2 emissions. For example, since 2017 the direct emissions of carbon from biomethane in France (23 gCO_2 / kWh) was about ten times less than the one from natural gas (244 gCO_2/kWh) [1], this explains the reason to prefer biomethane than natural gas. However, the price of biomethane in France (~ 100 €/MWh) is still higher compared to the price of natural gas (< 20 €/MWh) [6]**,** this is why many researches are increasingly conducted dealing with ways to reduce this price. Reducing the costs of biogas upgrading is one of ways to reduce the biomethane price. This work highlights the role of activated carbons (ACs) in biogas upgrading. Different technologies are known for biogas upgrading: Pressure Suing Adsorption (PSA), water scrubbing, amine scrubbing, membrane, cryogenic, and biological treatments. However, some of those technologies are pricey, others are energivores, and others emit chemicals enhancing climate-damaging. PSA technology is preferred due to its low costs and low energy requirements [7]. Moreover, PSA is based on the use of solid adsorbent materials such as activated carbons, zeolites, and metal organic frameworks to remove CO_2 via adsorption process; this makes it applicable over a wide range of temperatures and pressures [8]. Among adsorbents for CO_2 removal, activated carbons are considered as the best, thanks to their good textural properties, their good stability under acidic and basic conditions [9], their low costs, and their ease of regeneration [10]. ACs dispose high specific surface areas (400 - 3500 m^2/g) and large pores sizes (1.0 – 4.0 nm) [11], leading to high CO_2 adsorption capacity but low selectivity [12]. However, the selectivity of activated carbons can be optimized through surface modification (i.e. introducing chemical or/and physical materials) [13]. This work provides insight regarding the influence of activated carbons modification on CH_4 and CO_2 adsorption. For that concern, a homemade manometric setup was used, and a sufficient number of experiments were conducted on the adsorption of pure gases (CH_4 and CO_2) by commercial CNR-115 and two new modified activated carbons (CNR-115-ox and CNR-115-ox-am) at 303.15K and the pressure range of 0 - 3MPa. To describe the behavior of CH_4 and CO_2 on a set of activated carbons used, the Langmuir two parameters model was used and the results are well comparable to the ones are well comparable to the ones in the literature.

2 Materials and Methods

2.1 Commercial and New Modified Activated Carbons (Family of CNR-115)

Three activated carbons used in this work: commercial (CNR-115) and two new modified (CNR-115-ox and CNR-115-ox-am) were purchased at Mulhouse Materials Science Institute (IS2M, France). The surface chemistry of commercial CNR-115 was modified through two successive steps: a) oxidation under air at 400°C for 2h to increase the number of oxygenated groups. Activated carbon produced in this step is called CNR-115-ox, and b) ammonium vapor (NH_4OH) impregnation at 298K for 36h to increase the amount of nitrogenated groups. The resulted activated carbon in this step is called CNR-115-ox-am.

2.2 Activated Carbons Characterization

Textural properties of activated carbons were characterized by means of nitrogen adsorption/desorption measurements using a micrometrics ASAP2020 under 77K. BET (Brunauer, Emmet and Teller) model was used for specific surface area (SSA) determination. The total pore volume (V_t) was obtained for P/P_0 equals to 0.99. Dubinin-Radushkevich model was used to calculate the micropore volume (V_{micro}), whereas the mesopore volume (V_{meso}) was given by the difference between V_t and V_{micro}. SAIEUS software (Micromeritics) and 2D-NLDFT (Non Local Density Functional Theory [14]) were applied to determine the pore size distribution (PSD) which served in the average pore width (L_0) determination through the equation (1).

$$L_0 = \frac{1}{N}\sum_{i=1}^{N} \frac{w.dV/dW}{dV/dW} \quad (1)$$

Where, L_0 is the average pore diameter (nm), w is the pore width (nm), dV/dW is the differential pore volume per pore width ($cm^3\ nm^{-1}$), and N is the number of data points. The table 1 presents the textural properties obtained for activated carbons of the CNR-115 family: CNR-115, CNR-115-ox and CNR115-ox-am. In the table 1, it can be observed that the surface modification process remarkably reduces the BET surface of activated carbons of the CNR-115 family in the following sequence: CNR-115 (1714 $m^2\ g^{-1}$) > CNR-115-ox (929 $m^2\ g^{-1}$) > CNR-115-ox-am (352 $m^2\ g^{-1}$). The total pore volume has also decreased (more than half) after each modification process: CNR-115 (0.95 cm^2g^{-1}) > CNR-115-ox (0.45 cm^2g^{-1}) > CNR-115-ox-am (0.21 cm^2g^{-1}). Micro and meso-pore volumes, and average pore size were also impacted. However, the decrease in BET surface area is considered as normal result of modification process due to the fact that, the latter includes the temperature rise and thus the mass vaporization. The decrease in porosity can be associated with pore blockage that takes place during modification where the loading of oxygen and nitrogen functional groups may block some pores [15].

Table 1. Textural properties of CNR-115, CNR-115-ox and CNR115-ox-am [16].

Activated carbon	S_{BET} (m^2g^{-1})	V_{micro} (cm^3g^{-1})	V_{meso} (cm^3g^{-1})	V_{tot} (cm^3g^{-1})	L_0 (nm)
CNR-115	1714	0.64	0.31	0.95	1.10
CNR-115-ox	929	0.36	0.09	0.45	0.96
CNR-115-ox-am	352	0.14	0.07	0.21	0.78

On the other hand, the N_2 adsorption/desorption and 2D-NLDFT pore size distribution (figures 1 and 2 respectively) behave as type I isotherm because: i) the adsorbed volume increases at low pressures, and ii) there is the plateau formation at higher pressures.

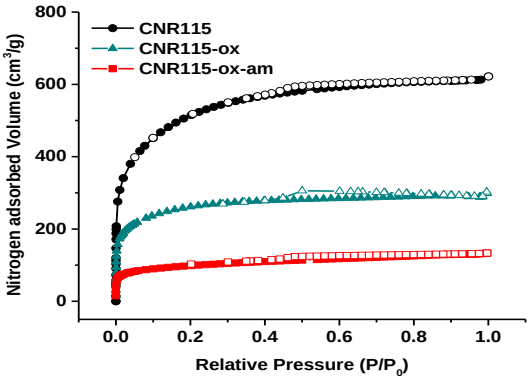

Figure 1. N_2 adsorption/desorption of CNR-115, CNR-115-ox and CNR-115-ox-am [16].

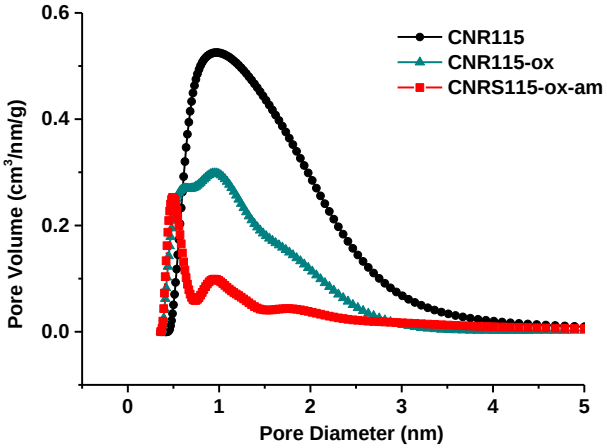

Figure 2. Pore size distribution of CNR-115, CNR-115-ox and CNR-115-ox-am [16].

2.3 Experimental System

Adsorption isotherms were determined by using manometric setup presented on the figure 3, at the temperature of 303.15K and the pressure range of 0 - 3MPa.

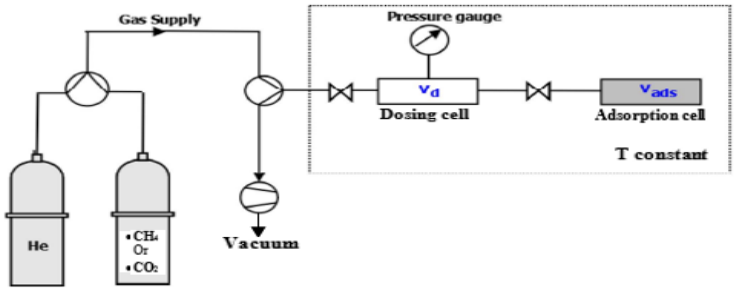

Figure 3. High-pressure manometric device for pure gases adsorption (adapted from [17]).

The system is composed of two basis elements which are the dosing and adsorption cells. To measure the pressure inside the cells, MKS pressure transducer baratron type 121 A (with 0.01% uncertainty from vacuum to 3.3 MPa) was used. The dosing and adsorption cells are separated by valves, whose also allow minimizing the dead space volume. Isothermal condition of the system was maintained at 303.15K by wrapping the cells with a heating wire controlled by a Eurotherm 3208 PID regulator, and was verified by using two thermocouples fixed on the cells. The system is also connected to the vacuum pump for regeneration process.

2.4 Volume Calibration

The dosing and adsorption cell volumes of the empty system were previously calculated by Deneb et al [17] by means of gravimetric calibration method, and the values obtained were 30.8 cm^3 and 19.05 cm^3 for dosing and adsorption volumes respectively. Determination of the volume occupied by adsorbent is then the preliminary step which must be done once a new mass of adsorbent sample is introduced into the system. This volume is slightly different from the one of the empty cell due to the fact that, the small volume is occupied by adsorbent. To do so, a small amount of activated carbon (~1g) was placed inside the adsorption cell (after vacuum at 90°C for 8h). When the isothermal conditions at the experimental temperature (303.15K) was reached, the small pressure of helium gas (i.e., inert gas which is not adsorbed by activated carbons) was introduced into the dosing cell. After the pressure stabilization, the initial pressure (P_i^i) was noted and the gas was expanded into the whole system [18]. At that stage, when the new stabilization of pressure was obtained, the final pressure (P_f^i) was taken and the first point (i=1) of the dead space volume (V_m) of adsorption cell was calculated by means of the ideal gas equation of state using the equation (2). Other doses of helium were then introduced successively in the dosing

cell and expanded into the adsorption cell. The dead-space volume for the i^{th} step was therefore expressed by using the equation (3), and the final dead space volume was given by the average of all the measurements.

$$V_m=V_d\left((P_i/P_f)-1\right) \quad (2)$$

$$V_m^i=V_d\left(\left(P_i^i-P_f^i\right)/\left(P_f^i-P_f^{i-1}\right)\right) \quad (3)$$

2.5 CH4 and CO2 Pure Gases Adsorption Measurements

To determine CH_4 and CO_2 pure gases adsorption isotherms, the main steps of experimental methodology are the following : i) a small activated carbon sample was measured and introduced directly into the adsorption cell. In this work, the amount of around 1g was chosen in order to get enough available adsorption area (50 m^2 is the minimum surface required) [19]. ii) The experimental system was regenerated under vacuum at 90°C for 8h in order to remove all the gases fixed at the surface of activated carbon. iii) The third step is to calculate the volume occupied by the adsorbent (as detailed above). iv) The experimental temperature (303.15K) was then settled. v) Lastly, the successive doses of gas (CH_4 or CO_2) were introduced and expanded into the dosing and adsorption cells respectively, and the initial and final pressures were noted after reaching the equilibrium. The number of adsorbed moles for the first point of the adsorption isotherm (n_{ads}^1) was calculated by using the equation 4, and the others points of the adsorption isotherm (n_{ads}^i) were given by the equation (5).

$$n_{ads}^1(T,P_1)=\left(V_d\rho_i\right)-\left((V_d+V_m)\rho_f\right) \quad (4)$$

$$n_{ads}^i(T,P_i)=\left(V_m\,\rho_f{}^{i-1}+V_d\rho_i{}^i\right)-\left((V_d+V_m).\rho_f{}^i\right) \quad (5)$$

Where, ρ_i and ρ_f (g cm^{-3}) are the molar density at initial and final pressures respectively. The values of ρ_i and ρ_f at the experimental temperature and pressures conditions were taken from the NIST (National Institute of Standards and Technology) database.

2.6 Langmuir Fitting Model

To study the adsorption behavior of pure CH_4 and CO_2 on the mentioned adsorbents, Langmuir two-parameter model (which takes into account the adsorbed phase) was used as in equation (6) [20].

$$n_{ads}^{excess}=n_L\frac{P}{P+P_L}\left(1-\frac{\rho_{g\,(P,T)}}{\rho_{ads}}\right) \quad (6)$$

Where n_{ads}^{excess} (mol kg^{-1}) is the amount of gas adsorbed at the working pressure P (MPa), P_L (MPa) is the Langmuir pressure, ρ_g (kg m^{-3}) is the gas density, and ρ_{ads} (kg m^{-3}) is the adsorbed phase density. In this work, the values of ρ_{ads} are fixed to be 1027 kg m^{-3} and 423 kg m^{-3} for CO_2 and CH_4 respectively [20]. The error of the fitting process (Δ_n)

was calculated through the standard deviation between experimental number of adsorbed moles and theoretical ones as in the equation (7).

$$\Delta_n = \frac{1}{N} \cdot \sqrt{\sum_{i=1}^{N} \left(n_{ads}^{exp} - n_{ads}^{FIT}\right)^2} \quad (7)$$

3 Results and Discussions

3.1 CH_4 and CO_2 Pure Gases Adsorption Isotherm

The figure 4 shows the results obtained for both CH_4 and CO_2 pure gases adsorption isotherms on CNR-115, CNR-115-ox and CNR-115-ox-am at 303.15K and the pressure range of 0-3MPa. The results highlight that, for the pressures ranging from zero to 3 MPa, activated carbons of CNR-115 family present higher adsorption capacities for CO_2 than for CH_4. Literately, this fact that carbon dioxide is highly adsorbed than methane, agrees with general behavior of activated carbons.

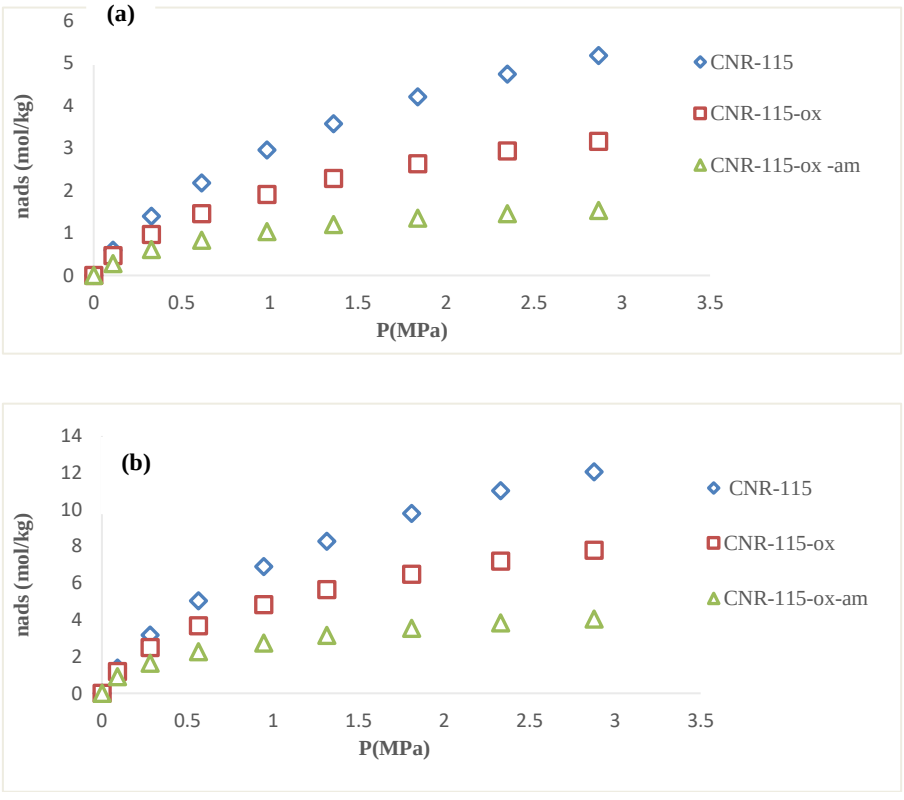

Figure 4. CH_4 (a) and CO_2 (b) pure gases adsorption isotherms on CNR-115, CNR-115-ox and CNR-115-ox-am at 303.15K.

Further possible explanations are based on the difference between CO_2 and CH_4 properties (table 2). From the table 2 it can be seen that; the kinetic diameter of carbon dioxide (330 pm) is less than that of methane (380 pm). When compared to the size of activated carbons of CNR-115 family as previously presented, carbon dioxide (i.e. the one with small size) will tend to be adsorbed than methane [21]. However, another reason is that, carbon dioxide doesn't present a dipole moment, but it contains unignorable quadrupole moment ($-13.7\times10^{40}cm^2$), this is contrary to methane which has no dipole or quadrupole moments. The higher the dipole and quadrupole moments, the greater the interactions gas–activated carbon [22]. In addition, a wider polarizability of CO_2 than CH_4 ($29.1\times10^{25}cm^3$ of CO_2 > $25.9\times10^{25}cm^3$ of CH_4) also explains the greatest interactions between CO_2 and activated carbons. Besides, the results also show a significant loss in adsorption capacity for both CH_4 and CO_2 from commercial CNR-115 to modified activated carbons. At 3Mpa, CO_2 adsorption capacity was in the following sequence: CNR-115 (12.05 $molk^{-1}$) > CNR-115-ox (7.79 $molkg^{-1}$) > CNR-115-ox-am (4.05 $molkg^{-1}$), and was the same order for CH_4 adsorption capacity: CNR-115 (5.18 $molkg^{-1}$) > CNR-115-ox (3.16 $molkg^{-1}$) > CNR-115-ox-am (1.53 $molkg^{-1}$). The highest CH_4 and CO_2 adsorption capacities of CNR-115 were surely related to its higher BET surface and higher pore volume. Those results were considered as accurate since the errors were very small ($\Delta_{nads} \leq 1\%$, $\Delta_T \leq 0.5\%$, and $\Delta_P = 1 - 5\ \%$).

Table 2. Properties of CH_4 and CO_2 molecules [23].

Property	CH_4	CO_2
Kinetic diameter (pm)	380	330
Dipole moment ($\times \mathbf{10^{-40}cm^2}$)	0	0
Quadrupole moment ($\times \mathbf{10^{-40}cm^2}$)	0	-13.7
Polarizability ($\times \mathbf{10^{-25}cm^3}$)	25.9	29.1

3.2 Langmuir Fitting

The table 3 shows the results obtained for the fitting of Langmuir model with CH_4 and CO_2 adsorption isotherms. The maximum Langmuir capacities of (8.45 $molkg^{-1}$ and 19.26 mol kg^{-1} for CH_4 and CO_2 respectively) were for unmodified activated carbon (CNR-115). This confirms the relationship between the adsorption capacity and the BET surface area (i.e. the greater the BET surface the higher the adsorption capacity).

Table 3. Langmuir parameters of CH_4 and CO_2 on activated carbons of CNR-115 family at 303.15K.

Sample	Components	$\mathbf{n_L}$ (mol kg^{-1})	$\mathbf{p_L}$ (MPa)	Δ_n
CNR-115	CH_4	8.45	1.79	0.003
	CO_2	19.26	1.68	0.073
CNR-115-ox	CH_4	4.78	1.53	0.040
	CO_2	9.71	0.94	0.120
CNR-115-ox-am	CH_4	2.10	1.04	0.030
	CO_2	4.39	0.57	0.010

It can also be observed in figure 5 that, the maximum Langmuir capacity was in good correlation with BET surface area, with good linear regression ($R^2 \geq 0.98$). However, the results were confirmed as reasonable and reproductive since the fitting error was small ($\Delta_n \leq 0.12$) for all the samples.

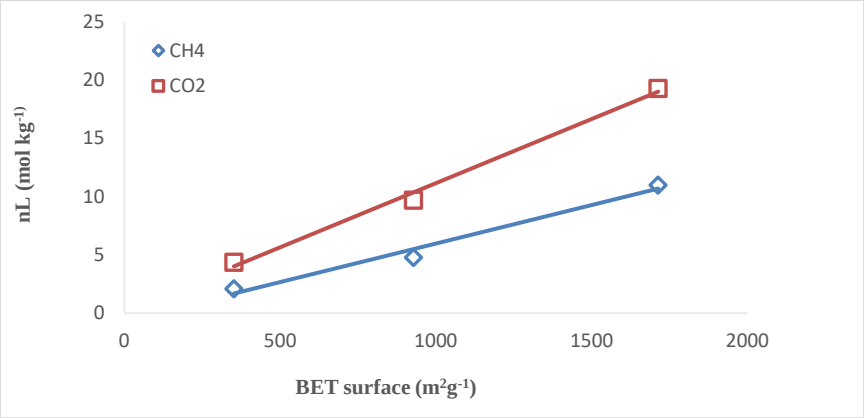

Figure 5. Maximum Langmuir capacity versus BET surface area of activated carbons of the CNR-115 family, at 303.15K

3.3 Interesting Side of CNR-115-ox-am: the New Modified Activated Carbon

The results discussed above highlight that CNR-115 adsorbs higher amount of both CH_4 and CO_2 compared to new modified activated carbons (CNR-115-ox and CNR-115-ox-am). However, the adsorption capacity is not the only one performance indicator of an adsorbent. The best one is therefore its selectivity (i.e. capacity to choose one component over another one from the mixture). For CH_4/CO_2 mixtures separation, an activated carbon which adsorbs the least CH_4 and moderated CO_2 can be preferred. This is because, CH_4 as the only one valuable component has to remain in the mixture for further uses [24]. In this study, the lowest CH_4 adsorption capacity (1.53 mmol/g) was obtained for CNR-115-ox-am, thus the reason to consider it as promising adsorbent for CH_4 enrichment from CH_4/CO_2 mixtures. This was already confirmed by the results of Deneb et al [16] who studied the adsorption of (CH_4/CO_2 50:50) mixture on CNR-115, CNR-115-ox and CNR-115-ox-am. According to their results, the selectivity of unmodified CNR-115 (< 2.7 through the whole pressure range) was almost 50 times less than the maximum selectivity value (129.0 at 2.17 MPa) for CNR-115-ox-am. Furthermore, when compared to the adsorption capacities from the literature as shown in table 4, methane adsorption capacity obtained in this work for CNR-115-ox-am at 303.15K and 0.1MPa (0.27 mol/g), is to the best of our knowledge among the lowest ones that are so far reported for activated carbons. Moreover, adsorption performances of CNR-115-ox-am are comparable to the ones reported for metal organic frameworks like (Cu-MOF) [25].

Table 4. CH_4 and CO_2 pure gases adsorption on different adsorbents, at 0.1 MPa.

Adsorbents	Modification process	BET (m^2/g)	T (K)	CH_4 uptake (mol/kg)	CO_2 uptake (mol/kg)	Ref.
CNR-115	-	1714	303	0.60	1.38	This work
CNR-115-ox	Air, 400°C	929	303	0.47	1.18	This work
CNR-115-ox-am	NH_4OH, 24h at 100°C	352	303	0.27	0.91	This work
GAC	-	865	273	-	4.66	[26]
GACO	HNO_3, 6hat 100 °C	787	273	-	5.38	[26]
GACA	NH_4OH, 24h at 100°C	634	273	-	7.57	[26]
Pitch-based	-	1457	303	1.10	2.50	[23]
Cu-MOF	-	105	298	0.47	0.86	[25]
Cu-MOF	-	105	318	0.35	0.65	[25]
MOF-1C	-	-	298	0.30	1.50	[27]

4 Conclusion

In this experimental study, CH_4 and CO_2 pure gases adsorption experiments were correctly conducted on commercial and modified activated carbons (family of CNR-115) at 303.15K and the pressure ranging from zero to three mega Pascals. Adsorption capacity of CO_2 was found to be higher than that of CH_4 for all the three activated carbons of CNR-115 family. A decrease in adsorption capacity was observed for both gases due to the decline in BET surface area and pore blockage which take place during modification process. Experimental isotherms were fitted to Langmuir two-parameter model in order to describe the behavior of adsorption process. Type I isotherm (i.e. monolayer adsorption) was therefore observed for CH_4 and CO_2 adsorption on a set of activated carbon of CNR-115 family. BET surface area was confirmed to be related to the adsorption capacity, and the values obtained are in good agreement with the ones reported in the literature [16],[28]. The modified activated carbon CNR-115-ox-am presents the advantage of adsorbing the least methane than other activated carbons of the CNR-115 family, which is thus the reason to consider this activated carbon as promising adsorbent for the future studies of CH_4 enrichment from CH_4/CO_2 mixtures.

Acknowledgments

The author would like to acknowledge the framework agreement between BIOCAD E_2S of Université de Pau et des Pays de l'Adour (UPPA), CATLP (Communauté d'Agglomeration Tarbes-Lourdes-Pyrénées), the French program ANR (ANR-16-IDEX-0002) and CARNOT ISIFOR for their financial support.

References

1. Gasquet V. Epuration d'H2S du biogaz à partir de résidus de traitement thermique bruts et formulés : Comparaison des performances et compréhension des mécanismes d'adsorption 223.
2. Vondra M, Touš M and Teng S Y 2019. Digestate evaporation treatment in biogas plants: A techno-economic assessment by Monte Carlo, neural networks and decision trees. *J. Clean. Prod.* **238** 117870.
3. Boulinguiez B and Le Cloirec P 2015. Purification de biogaz - Élimination des COV et des siloxanes. *Chim. Verte.*
4. Olivier T 2015. Étude technique, Économique et environnementale sur l'injection portée de biomethane dans le réseau de gaz.
5. Rogulska M, Bukrejewski P and Krasuska E 2018. *Biomethane as Transport Fuel.* (IntechOpen).
6. Tilagone R and Lecointe B 2015. Gaz naturel – Carburant pour véhicule 31
7. Kapoor R, Ghosh P, Kumar M and Vijay V K 2019. Evaluation of biogas upgrading technologies and future perspectives: a review. *Environ. Sci. Pollut. Res. Int.* **26** 11631–61.
8. Speight J G 2019. Chapter 15 - Hydrogen Production. *Heavy Oil Recovery and Upgrading* ed J G Speight (Gulf Professional Publishing) pp 657–97.
9. El-Shafey E I, Ali S N F, Al-Busafi S and Al-Lawati H A J 2016. Preparation and characterization of surface functionalized activated carbons from date palm leaflets and application for methylene blue removal. *J. Environ. Chem. Eng.* **4** 2713–24.
10. Pu Q, Zou J, Wang J, Lu S, Ning P, Huang L and Wang Q 2021. Systematic study of dynamic CO2 adsorption on activated carbons derived from different biomass. *J. Alloys Compd.* **887** 161406.
11. Sun L-M, Meunier F, Brodu N and Manero M-H 2016. Adsorption - Aspects théoriques
12. Ribeiro R, Sauer T, Lopes F, Moreira R, Grande C and Rodrigues A 2008. Adsorption of CO2, CH4, and N 2 in Activated Carbon Honeycomb Monolith. *J. Chem. Eng. Data - J CHEM ENG DATA* **53** 2311–7.
13. Zulkurnai N Z, Md. Ali U F, Ibrahim N and Abdul Manan N S 2017. Carbon Dioxide (CO_2) Adsorption by Activated Carbon Functionalized with Deep Eutectic Solvent (DES). *IOP Conf. Ser. Mater. Sci. Eng.* **206** 012001.
14. Jagiello J and Olivier J P 2013. 2D-NLDFT adsorption models for carbon slit-shaped pores with surface energetical heterogeneity and geometrical corrugation. *Carbon Complete* 70–80.
15. Madzaki H, KarimGhani W A W A B, NurZalikhaRebitanim, and AzilBahariAlias 2016. Carbon Dioxide Adsorption on Sawdust Biochar. *Procedia Eng.* **148** 718–25.
16. Peredo-Mancilla D, Hort C, Jeguirim M, Ghimbeu C M, Limousy L and Bessieres D 2018. Experimental Determination of the CH4 and CO2 Pure Gas Adsorption Isotherms on Different Activated Carbons. *J. Chem. Eng. Data* **63** 3027–34.
17. Peredo Mancilla J D 2019. *Adsorption and Separation of Carbon Dioxide for Biomethane Production: The Use of Activated Carbons.* Thèse de doctorat (Pau).
18. Bessières D, Lafitte T, Daridon J-L and Randzio S L 2005. High pressure thermal expansion of gases: Measurements and calibration. *Thermochim. Acta* **428** 25–30.
19. Mouahid A, Bessieres D, Plantier F and Pijaudier-Cabot G 2011. A thermostated coupled apparatus for the simultaneous determination of adsorption isotherms and differential enthalpies of adsorption at high pressure and high temperature. *J. Therm. Anal. Calorim.*.

20. Ortiz Cancino O P, Pino Pérez D, Pozo M and Bessieres D 2017. Adsorption of pure CO2 and a CO2/CH4 mixture on a black shale sample: Manometry and microcalorimetry measurements. *J. Pet. Sci. Eng.* **159** 307–13.
21. Cui A, Bustin R M and Dipple G 2004. Selective transport of CO2, CH4, and N2 in coals: Insights from modeling of experimental gas adsorption data. *Fuel* **83** 293–303.
22. Wu Y-J, Yang Y, Kong X-M, Li P, Yu J-G, Ribeiro A M and Rodrigues A E 2015. Adsorption of Pure and Binary CO $_2$, CH $_4$, and N $_2$ Gas Components on Activated Carbon Beads. *J. Chem. Eng. Data* **60** 2684–93.
23. Rodriguez-Reinoso F, Molina-Sabio M and Munecas M A 1992. Effect of microporosity and oxygen surface groups of activated carbon in the adsorption of molecules of different polarity. *J. Phys. Chem.* **96** 2707–13.
24. da Costa R B R, Valle R M, Hernández J J, Malaquias A C T, Coronado C J R and Pujatti F J P 2020. Experimental investigation on the potential of biogas/ethanol dual-fuel spark-ignition engine for power generation: Combustion, performance and pollutant emission analysis. *Appl. Energy* **261** 114438.
25. Giraldo L, Vargas D P and Moreno-Piraján J C 2020. Study of CO2 Adsorption on Chemically Modified Activated Carbon with Nitric Acid and Ammonium Aqueous. *Front. Chem.* **8** 543452.
26. Wu X, Yuan B, Bao Z and Deng S 2014. Adsorption of carbon dioxide, methane and nitrogen on an ultramicroporous copper metal–organic framework. *J. Colloid Interface Sci.* **430** 78–84.
27. Bae Y-S, Hauser B G, Farha O K, Hupp J T and Snurr R Q 2011. Enhancement of CO2/CH4 selectivity in metal-organic frameworks containing lithium cations. *Microporous Mesoporous Mater.* **141** 231–5.
28. Ho B N, Pino-Perez D, Matei Ghimbeu C, Diaz J, Peredo-Mancilla D, Hort C and Bessieres D 2021. Determination of methane, ethane and propane on activated carbons by experimental pressure swing adsorption method. *J. Nat. Gas Sci. Eng.* **95** 104124